J. Biomechanics Vol. 27, No. 2, pp. 177–181, 1994.
Printed in Great Britain

0021-9290/94 $6.00 + .00

THREE-DIMENSIONAL SIMULATIONS OF THE SCOLIOSIS DEROTATION MANEUVER WITH COTREL–DUBOUSSET INSTRUMENTATION*

MACK GARDNER-MORSE† and IAN A. F. STOKES
Department of Orthopaedics and Rehabilitation, University of Vermont, Burlington, VT 05405, U.S.A.

Abstract—The derotation maneuver using Cotrel–Dubousset instrumentation (CDI) is intended to correct the counterdirectional transverse plane rotations of the spine and of the vertebrae in thoracic scoliosis. This was simulated in a finite element model of an idealized thoracic scoliosis with an initial 65° scoliosis angle and 0° kyphosis angle. After 90° of rod rotation the apical vertebra derotated 50° towards the sagittal plane but the apical vertebra axial rotation worsened by 8°. The scoliosis angle corrected to 29° and a 54° kyphosis was created. If the initial rod curvature was reduced by 9°, the model predicted only small changes in spinal curvature resulting from the forces required to connect the vertebrae to the hooks. Decreased kyphosis and scoliosis curvatures but increased vertebra axial rotation were produced by the derotation maneuver. The increase in apical vertebra axial rotation was reversed by modifying the representation of the motion segments by repositioning their effective axes 30 mm posteriorly.

INTRODUCTION

For many years, surgical instrumentation for treating scoliosis was designed primarily to apply distraction forces to the spine. Recently, the design of Cotrel–Dubousset instrumentation (CDI) (Dubousset and Cotrel, 1991) has provided surgeons with new options. This instrumentation, and other similar designs, provides for application of a complex combination of forces to correct the spinal deformity, as well as providing increased rigidity of the final construct. In the CDI procedure, two curved rods are attached to the deformed spine by several hooks. For a right thoracic scoliosis (the most common curve pattern), the rod on the concave side of the scoliosis is applied first, then it is rotated and locked to the hooks. This is referred to as the *derotation maneuver*.

The derotation maneuver is intended to rotate the spine from its predominant plane of curvature in the frontal plane (scoliosis) into the sagittal plane, to produce a normal kyphosis and lordosis (Bridwell *et al.*, 1990). Thus, the plane of maximum curvature of the spine [plan d'élection (Peloux *et al.*, 1965)] is rotated in the same direction as the rod rotation (*spinal derotation*). Scoliosis deformity also involves transverse plane rotation of the vertebrae in the opposite direction for a curve in a kyphotic thoracic region (Stokes *et al.*, 1987). In order to derotate the vertebrae (*vertebral derotation*), moments in the opposite sense must be applied to the vertebrae (Fig. 1).

In this study we used an analytic model of a spine with idealized geometry to examine the biomechanics of the derotation maneuver. We addressed the question how both spinal derotation and vertebral derotation in opposite directions can be produced by the rotation of a single rod attached to the spine. In addition, we examined the sensitivity of the results to spinal curvature, rod curvature relative to spinal curvature, and to the model representation of the motion segments.

METHODS

The simplified surgical procedure analyzed here consists of three stages: fitting the curved rod to the hooks attached to the spine, rod rotation, and subsequent locking of hooks to the rod. These three stages in the CDI procedure were simulated in a finite element (FE) analysis. The model represented a thoracic spine with right convex scoliosis. It consisted of seven equally spaced vertebrae (six motion segments) in an idealized planar geometry (a half sine wave). Two scoliosis magnitudes (65 and 40° scoliosis angle), both with no curvature in the sagittal plane (Fig. 2), were studied. This combination of frontal plane curvature (scoliosis) and no sagittal plane curvature produced a plane of maximum curvature in the frontal plane. This occurs in severe scoliosis (Stokes *et al.*, 1987). The curve magnitudes used represent the range of scoliosis curvature normally operated on with CDI.

The thoracic motion segments were represented by motion segment beam elements (Gardner-Morse *et al.*, 1990) matched to experimentally derived measurement of the stiffness of the normal human thoracic motion segments (Panjabi *et al.*, 1976). The beam element representation was used because it permitted systematic modification of the segment properties. The principal axes of the motion segment beams were rotated in the transverse plane to match the measured vertebral axial rotation in idiopathic scoliosis of 0.45° per millimeter of lateral deviation from the spinal axis (Stokes *et al.*, 1987). This resulted in an initial 6 and

Received in final form 27 *May* 1993.
* Presented in part at the Second North American Congress on Biomechanics, Chicago, Illinois, U.S.A., 24–28 August 1992.
† Author to whom correspondence should be addressed.

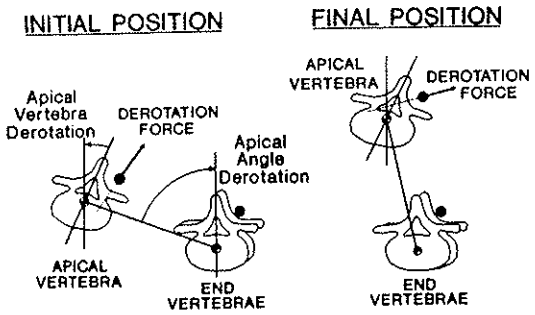

Fig. 1. In the initial position, the derotation force has a moment about the vertebral center tending to produce apical vertebral derotation. In the final position, the derotation force has a moment in the opposite direction about the center of the apical vertebra.

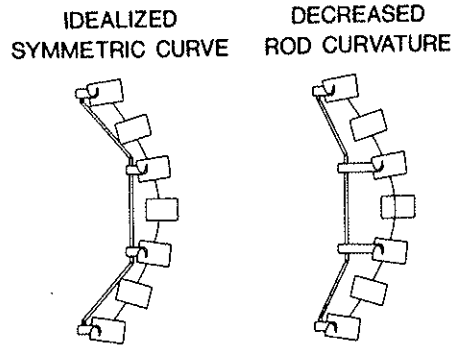

Fig. 2. The finite element model geometry with a single idealized scoliosis curve with the concave side rod. Left: 65° scoliosis angle model with equal curvature of the spine and rod. Right: decreased rod curvature by increasing the lateral distances of the hooks about the apical vertebra. The height of the spine is 120 mm and the lateral displacement of the apical vertebra is 25 and 14.2 mm for the 65 and 40° curves, respectively.

11° of rotation at the apical vertebra for the 40 and 65° scolioses, respectively.

The curved concave side rod of the CDI was represented by beam elements having properties corresponding to a 7 mm diameter steel rod (Fig. 2). The rod was connected to four of the vertebrae by hooks. The posterior part of each vertebra was represented by a stiff beam which provided a point of connection for a second stiff beam 10 mm long which represented the hook. Two hooks were connected to the end vertebrae and the other two hooks connected to the vertebrae on either side of the curve apex. This represented a typical arrangement of hooks used surgically. The connections between hooks and the rod were located 30 mm posterior and 10 mm towards the concave side of the curve relative to the local vertebral axis system. These dimensions were based on measurements of stereo X-rays of patients who has undergone the CDI procedure. The hooks were connected to the vertebrae by joints which allowed rotation about the lateral and posterior axes. The hooks were also free to rotate around the longitudinal axis of the rod until after 90° of rod rotation when the hooks were locked to the rod.

In the case of large scoliosis curves, surgeons use a rod curvature which is less than the scoliosis angle, in order to create a normal kyphosis curve after derotation. Therefore, a further simulation was performed with the 65° scoliosis angle model in which the rod curvature was decreased. This rod had a curvature of 51° compared to the original model's 60°, based on the enclosed angles between the two ends of the rod. To simulate the initial stage of the CDI procedure, in which the hooks are forcibly connected to a rod of lesser curvature, longer than normal hooks were used to connect the central two hooks to the rod. Then a thermal load (cooling) was applied to these hooks to reduce their lengths back to the original 10 mm length.

Based on the planar analysis of forces in Fig. 1, the position of the motion segment beam relative to the rod and hooks is important in determining both the magnitude and direction of the moment of the force applied to the vertebrae by the rod. In the initial position, a lateral offset of the motion segment neutral axis towards the curve concavity would decrease the apical vertebra derotation. In the final position, a posterior offset would increase the apical vertebra derotation. Therefore, the sensitivity of the model to lateral and posterior rigid offsets of the beam from its original position was investigated. Effects of offsetting the motion segment beams with 30 mm offsets in the lateral direction and 15 and 30 mm offsets in the posterior direction were examined.

Constraints (boundary conditions) were applied to maintain the equilibrium of the curved spine. The end vertebrae were only free to rotate in flexion–extension and lateral bending and translate in the vertical direction. Vertical translations were constrained at the apical (middle) vertebra. This represented almost a minimal set of constraints, in that it was only the restriction of axial rotation at both of the end vertebrae which exceeded the number of constraints necessary for the equilibrium of the model in response to external loading.

To simulate the derotation maneuver, the model input was a moment about the vertical axis applied to the midsection of the rod. *Rod rotation* was defined as the rotation of the ends of the rod about the longitudinal axis (Fig. 3). The nonlinear large displacement FE analysis was performed by a general purpose FE program (ANSYS, Swanson Analysis Systems, Inc., Houston, PA). In the derotation maneuver, after the rod rotation reached 90°, hook lock-up and subsequent release of the externally applied moment was simulated by making the rotational joint stiffnesses between the rod and the hooks extremely high, and then decreasing the applied moment until it reached zero.

To assess the results of this simulated derotation maneuver, four geometric measurements were defined (Fig. 3). The *scoliosis angle* was defined as the angle between normals at inflection points in the frontal plane projection of the line passing through vertebrae

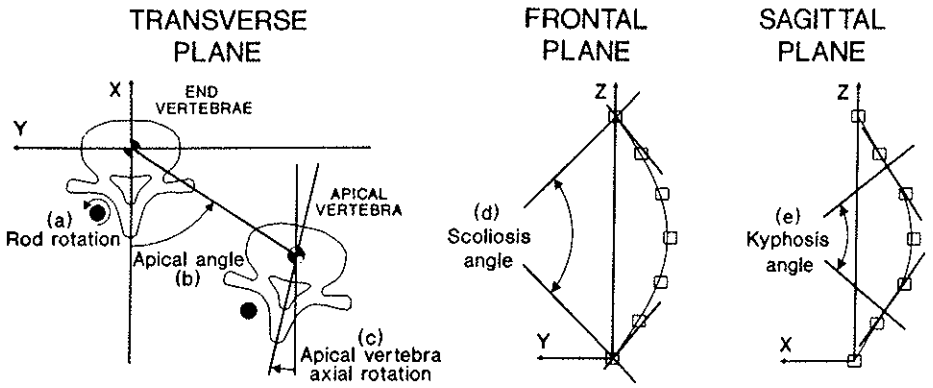

Fig. 3. Definition of terms used to quantify the results of the simulated surgery. Arrows show the directions of positive rotations: (a) rod rotation; (b) apical angle; (c) apical vertebra axial rotation; (d) scoliosis angle; (e) kyphosis angle.

Table 1. Initial model geometries and simulated results of the derotation maneuver

	Scoliosis angle (°)	Kyphosis angle (°)	Apical angle (°)	Apical vertebra axial rotation (°)	Peak torque (Nm)
Initial 65° scoliosis angle	65	0	90	11	–
No offset	29	54	40	19	6.5
15 mm posterior offset	26	54	38	16	7.8
30 mm posterior offset	19	52	31	8	7.9
30 mm lateral offset	27	51	40	13	9.9
Decreased rod curvature	25	38	49	22	4.6
Decreased rod curvature and 30 mm posterior offset	19	38	46	14	11
Initial 40° scoliosis angle	40	0	90	6	—
No offset	14	31	62	9	3.0
30 mm posterior offset	9	30	38	4	2.7

centers. The *kyphosis angle* was similarly defined as the angle between normals at inflection points in the sagittal plane projection. The *apical angle* was defined as an angular displacement of the apical vertebra from its normal position in the sagittal plane (DeSmet *et al.*, 1984). It is the angle between the A–P direction (X axis) and the line joining the apical vertebra's centroid to the Z axis passing through the end vertebrae. Spinal derotation was a reduction in apical angle. *Apical vertebra axial rotation* was defined as the rotation of the apex vertebra about its local z axis. Vertebral derotation was a reduction in apical vertebra axial rotation.

RESULTS

Spinal derotation of 50° occurred during the 90° rod rotation in the large scoliosis curve model (Table 1). However, vertebral rotation increased by 8° (Fig. 4). Thus, the simulated rod derotation maneuver decreased the spinal rotation, but increased the vertebral rotation. This pattern was similar for the smaller 40° scoliosis curve model (see Fig. 5). The change in vertebral rotation was sensitive to the representation of the motion segments, as expected from the planar analysis presented in Fig. 1. For the larger curve

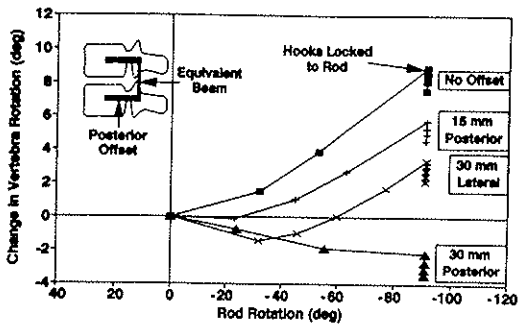

Fig. 4. Change in apical vertebral axial rotation as a function of rod rotation and motion segment representation. Results are shown for the 65° scoliosis angle model with 0, 15 and 30 mm posterior rigid offsets, and 30 mm lateral offset (towards the curve concavity) of the motion segment beams. The increase in vertebral rotation for the 0 mm posterior offset is contrary to the published reports which show a small decrease.

model, the 15 mm posterior offset produces 5° increase in apical vertebra axial rotation and with 30 mm posterior offset produced a 3° decrease (Fig. 4). Thus, a 30 mm posterior offset of the motion segment beams was required to produce both vertebral and spinal derotations.

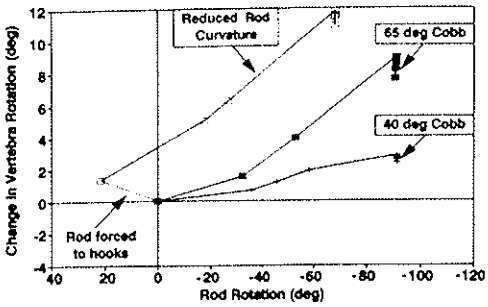

Fig. 5. Change in apical vertebral axial rotation as a function of rod rotation. Results are shown for the models with 40 and 65° scoliosis angle, and decreased rod curvature on the larger curve model. For the decreased rod curvature model there was an additional step in the simulation involving forcing the rod to attach to the hooks. The smaller initial scoliosis model had a disproportionately smaller increase in vertebral rotation. Reducing the rod curvature produced a greater increase in vertebral rotation.

The 30 mm lateral offset towards the curve concavity produced a small vertebral derotation during the initial stage of the derotation maneuver, but then the direction of apical vertebra axial rotation reversed to produce a final slight increase of 2°. For the larger initial curve the applied torque necessary for 90° of rod rotation increased with lateral or posterior offsets (Table 1).

In the decreased rod curvature model the hooks were first shortened to simulate elimination of the gap between the rod and the hooks. This produced negligible (< 1°) changes in spinal curvature but the apical vertebra axial rotation increased by 2°. After the derotation maneuver, apical vertebra axial rotation increased by a further 9° (Fig. 5). The apical angle decreased by 41° compared to 50° in the original model. Thus, there was less spinal derotation and a greater increase in the vertebral rotation.

DISCUSSION

This study was undertaken to investigate the biomechanics of the correction of two counterdirectional rotational components of scoliosis by the rotation of a rod connected to the spine. To correct these rotational deformities the rod rotation must produce spinal rotation in the same direction and apical vertebra rotation in the opposite direction (Fig. 1). The initial simulation failed to produce this effect. It only produced 50° derotation of the apical angle, and produced 8° of apical vertebral rotation in the wrong direction.

Consistent with the planar analysis of forces (Fig. 1), a model with rigid offset of the axes of the motion segment beams produced better agreement with reported surgical outcomes than models using published motion segment flexibility. The effect of such rigid offsets on a stiffness (or flexibility) matrix is given by the translation-of-axes transformations in Weaver and Gere (1980). Other changes to the beam properties would not have altered the stiffness ratio between forces and moments. Only models with 30 mm posterior offset produced vertebral derotation. The models with 0, 15 and 30 mm of posterior offsets showed that there is a nonlinear relationship between posterior offset and vertebral derotation. A possible anatomical reason why the rigid offsets provided a better match to measured changes is that the muscles omitted from this model provide additional stiffness posterior to the motion segments.

These models simulated the acute elastic changes resulting from the surgical maneuver of the concave side rod only, applied to an isolated spine without muscles or ribcage. The elastic properties of tissues were taken from the literature, which may not accurately reflect the *in vivo* properties of motion segments of an adolescent with scoliosis. These models do not include the uninstrumented spine; thus, questions about changes in compensatory curves (Kalen and Conklin, 1990) and spinal balance (Bridwell *et al.*, 1990; Mason and Carango, 1991; Moore *et al.*, 1991; Thompson *et al.*, 1990) were not investigated. The constraints (boundary conditions) on the models prevented any relative axial rotation between the end vertebrae. The biomechanics of the CDI procedure is complicated because it can also apply distraction forces which were not included in this simulation of the derotation maneuver alone. Also, it may be that the second (convex side) rod, which is often bent to a lesser curvature than the first rod, can be used to apply additional forces to the apical vertebra. These forces would tend to produce apical vertebra derotation, and to reduce the kyphosis angle.

Although the theory of the CDI is that it produces both spinal and vertebral derotations, published reports indicate that CDI has been more effective in producing spinal derotation than vertebral derotation. Pooled data from Cundy *et al.* (1990) and Ecker *et al.* (1988) show an average preoperative Cobb angle of 50° which corrected to 17° postoperatively (66% correction). However, the average preoperative apical vertebra rotation of 14° only corrected to 11° postoperatively (20% correction) as measured by CT scans. Wood *et al.* (1991) reported only an average 9% correction in vertebral rotation when it was referenced to the pelvis. Similarly, Gray *et al.* (1991) found intraoperatively that the derotation of the apical vertebra was negligible compared to that of a neutral vertebra. The models presented here show a similar correction for the scoliosis angle (55 and 65% correction in the large and small curve models, respectively) but there was only a small decrease in vertebral rotation in the simulations with 30 mm posterior offsets.

These simulations do provide some practical insights for surgeons planning CDI surgery. First, it may be possible to control the relative amounts of spinal and apical vertebra derotation as well as maximum forces exerted during surgery by using rods of different curvature. Second, the AP distance from motion segments to the point where hooks apply forces to

vertebrae should be minimized in order to minimize the tendency of the derotational forces to increase the apical vertebra axial rotation.

Acknowledgements—Supported by NIH R01 AR 40093. The authors thank Drs David Aronsson, M.D. and Jeffrey P. Laible, Ph.D. for their helpful discussions.

REFERENCES

Bridwell, K. H., Betz, R., Capelli, A. M., Huss, G. and Harvey, C. (1990) Sagittal plane analysis in idiopathic scoliosis patients treated with Cotrel–Dubousset instrumentation. *Spine* **15,** 644–649; 921–926.

Bridwell, K. H., McAllister, J. W., Betz, R. R., Huss, G., Clancy, M. and Schoenecker, P. L. (1991) Coronal decompensation produced by Cotrel–Dubousset "derotation" maneuver for idiopathic right thoracic scoliosis. *Spine* **16,** 769–777.

Cundy, P. J., Paterson, D. C., Hillier, T. M., Sutherland, A. D., Stephen, J. P. and Foster, B. K. (1990) Cotrel–Dubousset instrumentation and vertebral rotation in adolescent idiopathic scoliosis. *J. Bone Jt Surg.* **72B,** 670–674.

DeSmet, A. A., Asher, M. A., Cook, L. T., Goin, J. E., Scheuch, H. and Orrick, J. M. (1984) Three dimensional analysis of right thoracic idiopathic scoliosis. *Spine* **9,** 377–381.

Dubousset, J. and Cotrel, Y. (1991) Application technique of Cotrel–Dubousset instrumentation for scoliosis deformities. *Clin. Orthop.* **264,** 103–110.

Ecker, M. L., Betz, R. R., Trent, P. S., Mahboubi, S., Mesgarzadeh, M., Bonakdapour, A., Drummond, D. S. and Clancy, M. (1988) Computer tomography evaluation of Cotrel–Dubousset instrumentation in idiopathic scoliosis. *Spine* **13,** 1141–1144.

Gardner-Morse, M. G., Laible, J. P. and Stokes, I. A. F. (1990) Incorporation of spinal flexibility measurements into finite element analysis. *J. biomech. Engng* **112,** 481–483.

Gray, J. M., Smith, B. W., Ashley, R. K., LaGrone, M. O. and Mall, J. (1991) Derotational analysis of Cotrel–Dubousset instrumentation in idiopathic scoliosis. *Spine* **16,** S391–S393.

Kalen, V. and Conklin, M. (1990) The behavior of the unfused lumbar curve following selective thoracic fusion for idiopathic scoliosis. *Spine* **15,** 271–274.

Mason, D. E. and Carango, P. (1991) Spinal decompensation in Cotrel–Dubousset instrumentation. *Spine* **16,** S394–S403.

Moore, M. R., Baynham, G. C., Brown, C. W., Donaldson, D. H. and Odom, J. A. Jr. (1991) Analysis of factors related to truncal decompensation following Cotrel–Dubousset instrumentation. *J. spinal Disord.* **4,** 188–192.

Panjabi, M. M., Brand, R. A. and White, A. A. (1976) Three dimensional flexibility and stiffness properties of the human thoracic spine. *J. Biomechanics* **9,** 185–192.

Peloux, J. du, Fauchet, R., Faucon, B. and Stagnara, P. (1965) Le plan d'election pour l'examen radiologique des cyphoscolioses. *Rev. Chir. Orthop.* **51,** 517–524.

Stokes, I. A. F., Bigalow, L. C. and Moreland, M. S. (1987) Three-dimensional spinal curvature in idiopathic scoliosis. *J. Orthop. Res.* **5,** 102–113.

Thompson, J. P., Transfeldt, E. E., Bradford, D. S., Ogilvie, J. W. and Boachie-Adje, O. (1990) Decompensation after Cotrel–Dubousset instrumentation of idiopathic scoliosis. *Spine* **15,** 927–931.

Weaver, W. Jr. and Gere, J. M. (1980) *Matrix Analysis of Framed Structures*, pp. 383–417. Van Nostrand, New York.

Wood, K. B., Transfeldt, E. E., Ogilvie, J. W., Schendel, M. J. and Bradford, D. S. (1991) Rotational changes of the vertebral-pelvic axis following Cotrel–Dubousset instrumentation. *Spine* **16,** S404–S408.